THE JOURNAL OF PHYSICAL CHEMISTRY C

pubs.acs.org/JPCC Article

Hydrogen-Bonded Tetramers of Carbamazepine

Angela M. Silski-Devlin, Jacob P. Petersen, Jonathan Liu, Gwendylan A. Turner, John C. Poutsma, and S. Alex Kandel*

Cite This: J. Phys. Chem. C 2020, 124, 5213−5219 Read Online

ACCESS | Metrics & More | Article Recommendations | Supporting Information

ABSTRACT: In this study, the pharmaceutical carbamazepine (CBZ) and the related molecule dibenzazepine (DBZ) are prepared on the Au(111) surface and visualized using scanning tunneling microscopy. Monolayers of CBZ consist of tetrameric clusters that are highly ordered, while a monolayer of the molecular analog in which the amide group is removed, DBZ, consists of disordered clustering. Electrospray ionization mass spectra of CBZ show a relatively intense tetramer peak that is roughly six times more intense than the trimer peak, indicating the anomalous stability of a four-molecule cluster. The mass spectrum of DBZ shows relatively little clustering and does not show preference for tetramers. Our molecular modeling suggests that the CBZ tetramer is a NH···O hydrogen-bonded cluster, with reinforcing $\pi\cdots\pi$ interactions between benzene rings of neighboring molecules, which are responsible for the long-range order of the tetramers.

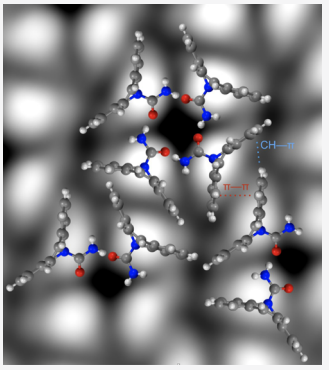

INTRODUCTION

Polymorphism is the existence of multiple different crystal packing arrangements for a given molecule, and different crystal polymorphs can exhibit different physical properties. Of these, solubility (and as a consequence, bioavailability) of different polymorphs is of particular interest to the pharmaceutical industry. Active pharmaceutical ingredients (APIs) are typically required to be polymorphically pure in order to achieve approval by the Food and Drug Administration in the US. However, identifying all of the polymorphs of a given compound is a difficult task, whether done experimentally or computationally.[1,2]

Polymorphic impurity in the pharmaceutical industry is a serious issue that in several cases has caused a drug to be removed from the market. Ritonavir, an API used in AIDS medications, was removed from the US drug market in 1998 because of the discovery of a second polymorph that precipitated out of gel capsules because of decreased solubility.[3,4] In addition, researchers failed to reproduce form I of ritonavir; this was labeled as a case of "disappearing polymorphs.[2] Almost a decade later, rotigotine, an API that is used in a skin patch to treat Parkinson's disease, was pulled off the US drug market in 2007 because of the unexpected discovery of a second polymorph that could not be absorbed by the skin.[5,6] These cases demonstrate the severity of polymorphic impurity and how controlling the formation of a particular polymorph can be difficult to accomplish.

Crystal structures in both two and three dimensions are difficult to predict a priori, solely based off of the structure of the starting molecule.[7] It is especially difficult to predict the supramolecular packing of molecules with more than one functional group that is capable of hydrogen bonding.[8] Crystal structure prediction has advanced in recent decades, and recent "blind" tests have demonstrated that crystal structures of organic crystals can be predicted,[9] but this remains at the cutting edge of molecular modeling and electronic structure calculations. In addition, current crystal structure prediction methods tend to neglect templating effects and kinetic factors, which can play a significant role in dictating crystallization pathways, and which may result in the formation of metastable, kinetically trapped structures.[10] There have been even fewer efforts to rationally predict the self-assembly of crystals in two dimensions.[11]

Carbamazepine (CBZ) is an API used to treat epilepsy. CBZ has five known anhydrous polymorphs, four of which commonly occur and are based on the amide-dimer motif,[12,13] and one that crystallizes less commonly and is based on a catemer motif.[14] Only one of these polymorphs is approved as an active pharmaceutical. Given that CBZ is highly polymorphic, we deemed this molecule a good candidate for this fundamental study of polymorphism and the early stages of crystallization. Scanning tunneling microscopy (STM), with its submolecular resolution, provides the ability to elucidate the early stages of the crystallization process, which may provide insight into the crystallization conditions required for the formation of different polymorphs. There have been few STM studies of active pharmaceut-

Received: December 11, 2019
Revised: January 21, 2020
Published: February 13, 2020

https://dx.doi.org/10.1021/acs.jpcc.9b11466
J. Phys. Chem. C 2020, 124, 5213−5219

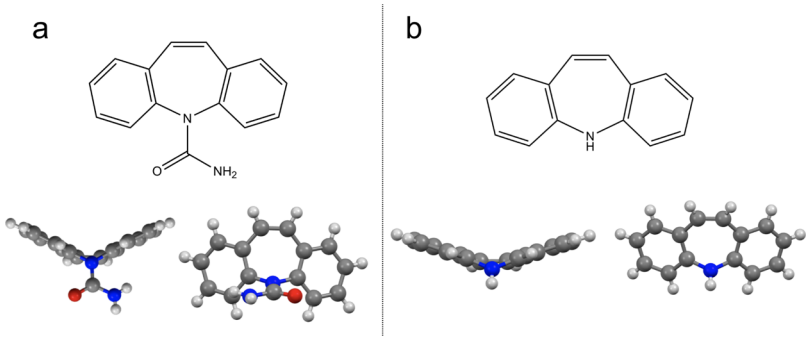

Figure 1. Chemical structure and ball-and-stick models of (a) CBZ and (b) DBZ. Both molecules have a "bowed" molecular geometry.

icals,[15−17] but we believe that studies of the self-assembly of APIs may improve the field of crystal structure prediction.

Previously, the Sykes group had imaged monolayers of CBZ molecules vapor-deposited on Au(111) and Cu(111) surfaces, both of which resulted in the formation of trimer clusters of CBZ molecules.[16] Herein, we discuss a combined STM and electrospray ionization mass spectrometry (ESI−MS) study of the clustering behavior of CBZ and an analog molecule, dibenzazepine (DBZ), in which the amide group is removed. We show that CBZ forms an unusual packing of tetrameric clusters that are highly ordered within a network upon solution deposition on the Au(111) substrate. The mass spectrum of CBZ consists of an anomalously intense tetramer peak, which points to the anomalous stability associated with four molecules per cluster. A monolayer of DBZ does not have readily apparent order, and the mass spectrum does not show a preference for a tetramer, which suggests that the CBZ tetramer is likely supported by hydrogen bonds of the amide groups. The difference in monolayer structures between the experiments we present here and the Sykes group studies (which are prepared at different substrate temperatures and different molecular deposition techniques) illustrates that there are multiple kinetic pathways to the self-assembly of CBZ molecules.

METHODS

Scanning Tunneling Microscopy. Au(111)-on-mica substrates were cleaned in high vacuum with three cycles of Ar^+ sputtering (0.55 kV for 15 min) and annealing at 350−400 °C. Substrates were allowed to cool before transferring to a load-lock chamber for preparation of the monolayer. Solutions of CBZ and DBZ (10 mM, Sigma-Aldrich, used without further purification) in acetonitrile and methanol were prepared. Droplets of the solutions of the molecule of interest were delivered via a pulsed-solenoid valve (Parker Instruments, Series 9, Iota One Driver, 0.5 mm diameter nozzle) onto the cleaned Au(111) substrate kept at room temperature in a load-lock chamber. The sample was then transferred to an Omicron LT-STM, kept at a base pressure of 5×10^{-10} Torr, and was cooled to 77 K. All images were acquired with a Pt/Ir tip in the constant current mode with a tunneling current of 10 pA and a tip−sample bias of +1.0 V (unless otherwise noted). All images presented are unfiltered, with the exception of Figure 2d, in which anomalously noisy scan lines were replaced with median-filtered pixels.

Electrospray Ionization Mass Spectrometry. All ESI−MS experiments were done using a Waters ACQUITY tandem triple quadrupole mass spectrometer equipped with a ZSpray electrospray ionization source. Solvated analyte solutions were injected into the electrospray capillary via a syringe pump (Harvard Scientific) at a flow rate of 10 μL/min. Spectra were collected in the positive ion mode. The electrospray source conditions were chosen in order to maximize ion transmission and to minimize the dissociation of molecular cluster ions, and they are listed with the spectra. Individual scan time was typically 3 s; spectra were acquired for 3 min.

RESULTS AND DISCUSSION

STM Images. Solution deposition of CBZ on Au(111) results in a monolayer that consists almost entirely of tetrameric clusters that are ordered as part of a network, as shown in Figure 2a,b. As the composite image in Figure 2c illustrates, the repeating tetramer unit is square, with each molecular feature appearing roughly triangular and containing a bright spot in the center surrounded by dim features. Given that features in STM images are a convolution of topography and electron density, it can be difficult to assign these features to different functional groups of the molecule, especially when the molecule is not planar (Figure 1).

CBZ was solution-deposited in methanol in order to probe the role of solvent dependence in the formation of tetramers (Figure 2d). Tetramers of CBZ are also observed as a result of solution deposition in methanol, although the internal structure of the tetramers appears to be different. Methanol, a hydrogen-bond-capable solvent, may interact with CBZ molecules in a way that acetonitrile does not, which could be the reason for the difference in the structure. Nonetheless, tetramers are formed in both acetonitrile and methanol.

This pattern of repeated tetramers of CBZ molecules on the Au(111) surface which we observe is rather different from the trimeric CBZ clusters that the Sykes group has previously observed on the Au(111) surface.[16] The difference in monolayer structures may be attributed to sample preparation conditions: the Sykes group prepared the monolayer of CBZ via vapor deposition and the substrate was held at 78 K, whereas the data we present in Figure 2 are obtained by solution deposition at room temperature. Solution deposition has been known to result in metastable configurations, as compared to vapor-deposited monolayers of the same molecule.[18,19] In addition, because there is less thermal energy available at 78 K than at room temperature, adsorbate molecules have less energy to re-organize into a lower energy configuration, and the resulting trimer structure may be a metastable configuration that at higher temperature, could re-organize into a different configuration, in this case, tetramers.

An anomalous cluster such as a four-molecule cluster is likely held together by hydrogen-bonding interactions because of their strength and directionality. Hydrogen-bonding inter-

https://dx.doi.org/10.1021/acs.jpcc.9b11466
J. Phys. Chem. C 2020, 124, 5213−5219

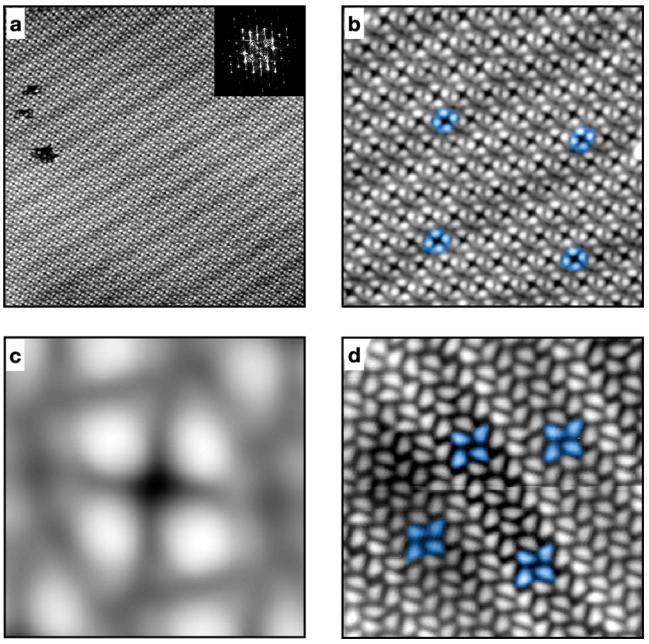

Figure 2. STM images of a monolayer of CBZ on Au(111) prepared by solution deposition in acetonitrile. (a) Large-scale STM image of CBZ molecule packing in an ordered network. 500 × 500 Å^2 area. Inset: two-dimensional fast Fourier transform. (b) 200 × 200 Å^2 area with representative tetramer structures highlighted in blue. (c) 20 × 20 Å^2 composite image of 181 tetramers shown in panel (b). (d) 116 × 116 Å^2 area of CBZ solution-deposited in methanol, with representative tetramers in blue (V_b = +1.0 V, tunneling current = 20 pA).

actions can provide the energetic stability required to overcome the energetically unfavorable steric interactions that are associated with adding more molecules to a cluster. There are several reported examples of tetrameric clusters stabilized by both strong and weak hydrogen bonds.[20−23] The ordered tetramer networks (quadruplexes) of xanthine molecules on Au(111) are held together by hydrogen bonds.[23] However, given that CBZ has only one hydrogen-bond acceptor group, it is unlikely that hydrogen bonding is responsible for both the formation of the tetramer clusters and the ordered packing of the tetramer clusters.

In order for the amide groups on the CBZ molecule to be close enough to form hydrogen bonds, we propose that the molecule is lying on its side such that the amide groups point to the center of the cluster to form cyclic NH···O hydrogen bonds. In Figure 3, molecular models of a hydrogen-bonded tetramer cluster are overlaid onto our STM images. The proposed hydrogen-bonded structure in Figure 3 may illustrate how the CBZ tetramer clusters pack together in long-range order, which may be the result of CH···π and π···π contacts between the DBZ rings of each CBZ molecule. Otherwise, if each CBZ molecule adsorbed on the surface is in the "standing-up" position (in which the DBZ rings are in contact with the surface and the amide group is pointing upward), the hydrogen-bond-capable functional groups would not be close enough to form hydrogen bonds to form the tetramer and the DBZ rings of neighboring molecules would be too closely packed to allow for the formation of the ordered networks of tetramers.

In interest of testing our proposed hydrogen-bonding CBZ tetramer structure, we performed STM experiments on the

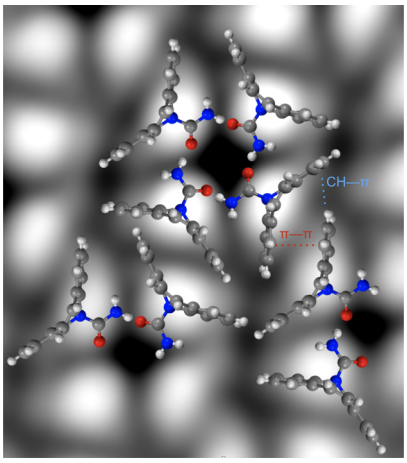

Figure 3. Molecular model of CBZ molecules overlaid onto STM data.

DBZ molecule (structure shown in Figure 1b) in which the amide group is removed from CBZ. This analog molecule no longer has a strong hydrogen-bond acceptor group, and thus, we would expect hydrogen-bonding interactions to be less influential in the formation of the DBZ monolayer. Figure 4a,b

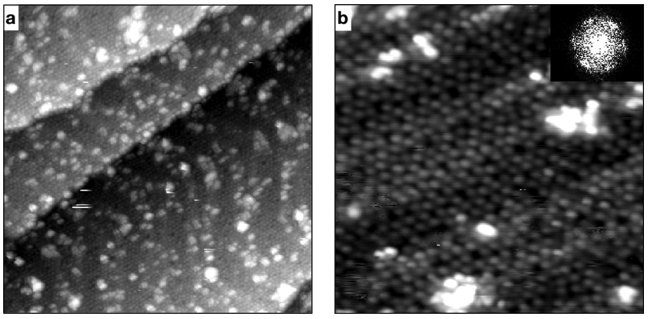

Figure 4. STM images of a monolayer of DBZ solution-deposited on Au(111) showing molecules clustering in no apparent order. (a) 500 × 500 Å^2 area near step edges. (b) 150 × 150 Å^2 area. Inset: Fourier transform of image (b).

shows STM images of a monolayer of DBZ solution-deposited on Au(111). Unlike CBZ, a monolayer of DBZ does not consist of long-range tetramer networks but rather consists of molecules packing with no readily apparent order. Although the DBZ monolayer structure (if any) is unclear, it is apparent that there is no long-range tetramer ordered network, as was the case for CBZ. The inset of Figure 4b shows the two-dimensional Fourier transform of the DBZ monolayer, which illustrates that there is no long-range order to the monolayer. The absence of tetramer networks in the DBZ monolayer suggests that the amide group is necessary to stabilize the CBZ tetramer cluster because the removal of the amide group precludes the formation of tetramers.

Gas-Phase Ion Studies in Mass Spectrometry. ESI is a "soft" ionization technique that keeps larger cluster aggregates intact, allowing for the study of gas-phase ion clustering.[24] ESI has been an effective tool in identifying and characterizing metastable clusters, which are typically revealed in a mass spectrum as peaks with a greater relative intensity compared to neighboring peaks.[25−29] Such metastable clusters, or the so-called "magic-number" clusters, are a configuration of atoms or molecules that exhibit unusual enhanced stability.

https://dx.doi.org/10.1021/acs.jpcc.9b11466
J. Phys. Chem. C 2020, 124, 5213−5219

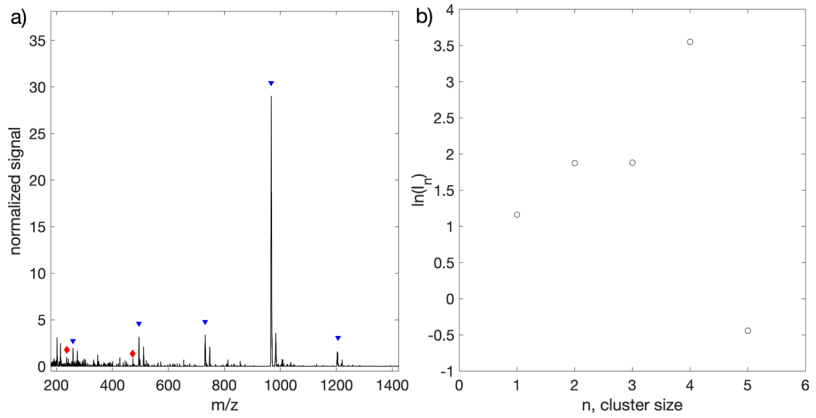

Figure 5. (a) Positive ion mode ESI−MS spectrum of CBZ in acetonitrile with a capillary and cone voltage of 4.0 kV and 10 V, respectively. The peak position that corresponds to the $[(CBZ)_n + Na]^+$ peaks for n = 1−5 is indicated by a blue triangle and that for $[(CBZ)_n + H]^+$ peaks for n = 1−2 is indicated by a red diamond. The signal is normalized to the monomer peak. (b) Natural log plot of the integrated intensity of each $[(CBZ)_n + Na]^+$ peak.

A positive ion mode mass spectrum of a 2 mM solution of CBZ in acetonitrile is shown in Figure 5a. The mass spectrum reveals relatively small $[(CBZ)_n + H]^+$ peaks, with $[(CBZ)_n + Na]^+$ peaks being the majority species for each family of n cluster size peaks for n = 1−6. Typically, in ESI, there is an exponential decay of signal abundance with an increased size of aggregates. However, a natural log plot of the integrated intensity of the $[(CBZ)_n + Na]^+$ peaks (Figure 5b) illustrates that CBZ clusters do not follow an exponential decay (which would be indicated by a linear negatively sloped fit). The signal abundance of $[(CBZ)_n + Na]^+$ peaks increases with cluster size until n = 4, which is roughly six times larger than the signal intensity of the n = 3 peak. Instrument conditions for the spectrum acquired in Figure 5a were adjusted to be gentle (i.e., lower cone voltage) to maximize abundance of the higher n clusters.

Tetramers are present both as anomalously large peaks in the mass spectrum and as the predominant building block of surface monolayers observed by STM. This follows a number of previous experiments from our laboratory which show agreement between the size of surface-adsorbed clusters with "magic-number" peak intensities in ESI−MS.[28,29] We suggest that the concordance between two very different experimental measurements is evidence that the CBZ tetramers are forming in solution and then (depending on the experiment) either delivered to the surface intact through solution deposition or ionized intact through electrospray.

It remains an open question, however, whether tetramers are present to some extent in all solutions or whether they are formed under the high-concentration, nonequilibrium conditions present in evaporating droplets. The literature is not decisive as to whether or not electrospray mass spectra are reflective of gas-phase or solution-phase behavior. The lanthanide chloride clusters are an example of "magic-number" clusters that are proposed to form as a result of ESI, given that there was an enhancement in the magic-number cluster peak upon dilution.[30] It would be expected that if clusters are formed in solution, upon dilution, the signal would decrease uniformly, and the relative ratios of peak intensities would remain the same under the given electrospray conditions. In addition, fluorescence excitation studies of octaethylporphyrin show that the gas-phase ion behavior is not reflective of the solution-phase ion intensities of the electrosprayed solution.[31]

Given the debate if gas-phase ion behavior or solution-phase behavior is reflective in the mass spectrum of a given molecule, it may be difficult to discern with certainty the mechanism of formation of the "magic" CBZ tetramer clusters. However, given that we observe tetramers of CBZ solution-deposited on the Au(111) surface as well, we posit that the electrosprayed plume is not required to form the tetramer structures as the monolayer of tetramers we observe was not prepared via electrospray deposition.

In order to test if the relative intensity of $[(CBZ)_4 + Na]^+$ is a function of concentration of the analyte, ESI−MS experiments were performed in a range of concentrations from 2 mM to 30 μM in both acetonitrile (SI Figures S1−S5) and methanol (SI Figures S6−S12). As the concentration of the CBZ solutions decreases, the relative ratio of peak intensities of tetramer to trimer gradually decreases (Tables S1 and S2). However, the $[(CBZ)_4 + Na]^+$ peak still remains "magic" at 30 μM in acetonitrile (Figure S5), while in methanol, the tetramer peak is no longer more intense than the trimer peak at 30 μM (Figure S12). Tables S3 and S4 display the scaled intensities (I_n) for the tetramer peaks, which are calculated relative to both neighboring peaks; these scaled intensities for the tetramer peak are overall higher in acetonitrile than in methanol, but in both solvents, the tetramer peak is considered "magic" (where $I_n > 1$).[32,33] The persistence of the anomalously intense tetramer peak at lower concentrations indicates that the "magic-number" tetramer is not simply a concentration phenomenon. The anomalously intense tetramer peak is also not a solvent phenomenon as the intense tetramer peak remains in methanol. While Rutkowski and co-workers[30] suggest that an increase in the relative peak intensities upon dilution points to the formation of the clusters as a result of ESI, we observe the opposite trend in our experiments. This suggests that the tetramers are not formed via ESI.

We considered the possibility that the presence of the "magic" tetramer peak is a function of electrospray conditions. In order to test this, we performed experiments at a variety of cone voltages. At higher cone voltages, there is still an increase of signal intensity with cluster size until n = 3, which is roughly equal in peak intensity to n = 4 (Figure S13). It is plausible that at higher cone voltages, the $[(CBZ)_4 + Na]^+$ peak does not remain intact and fragments into $[(CBZ)_3 + Na]^+$ via neutral loss of a CBZ monomer. MS/MS mode product scans

https://dx.doi.org/10.1021/acs.jpcc.9b11466
J. Phys. Chem. C 2020, 124, 5213−5219

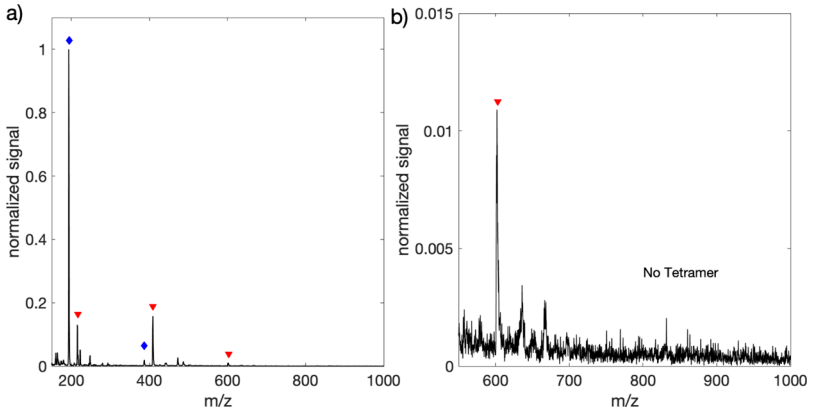

Figure 6. (a) Positive ion mode ESI−MS spectrum of DBZ in methanol with a capillary and cone voltage of 4.0 kV and 20 V, respectively. The $[(DBZ)_n + H]^+$ peaks for n = 1−2 are indicated by a blue diamond and $[(DBZ)_n + Na]^+$ peaks for n = 1−3 are indicated by a red triangle. The signal was normalized to the monomer peak. (b) Close-up view of the mass spectrum shown in (a) with a mass range of 550−900 m/z to show that there was no $[(DBZ)_4 + H]^+$ or $[(DBZ)_4 + Na]^+$ peak in the mass spectrum of DBZ, which would be expected to appear at roughly 773 and 796 m/z, respectively.

of the $[(CBZ)_4 + Na]^+$ peak reveal that the descendant peaks are primarily $[(CBZ)_2 + Na]^+$ and $[(CBZ)_3 + Na]^+$ (Figure S14). Although the relative ratio of the tetramer to trimer peak changes at different cone voltages, there remains a greater intensity of the tetramer than what would be expected with an exponential decay of signal intensity with increasing cluster size.

It is also possible that the presence of Na^+ in our instrument may influence the stabilization of the "magic" tetramer cluster. While Na^+ ions are difficult to remove from our public instrument, collaborators of ours performed experiments on a Thermo LTQ-Quantum Ultra triple quadrupole instrument equipped with a field asymmetric ion mobility spectroscopy source, and the results are shown in Figure S10. The spectrum in Figure S15 does show the presence of Na^+ ions, albeit to a lesser degree. We cannot explicitly rule out the possibility that Na^+ plays a role in the stabilization of the CBZ tetramer, given that various electrospray conditions and concentrations and a different instrument all resulted in the presence of a $[(CBZ)_4 + Na]^+$ peak with anomalous intensity. However, given the presence of tetramer networks on the Au(111) surface prepared by solution deposition, in the absence of sodium ions present in mass spectrometers, the sodium ion is not required for the formation of tetramer clusters.

A mass spectrum of the DBZ analog molecule (structure in Figure 1b) has poor signal-to-noise ratio in acetonitrile (Figure S15) and few peaks were resolved. A mass spectrum of DBZ was acquired in methanol (which has a better ionization efficiency than acetonitrile in ESI because of methanol's ability to donate a proton) and the spectrum does not show enhanced stability for n = 4 molecules under the same electrospray conditions. The mass spectrum (Figure 6a) includes $[(DBZ)_n + H]^+$ peaks for n = 1−2, in addition to $[(DBZ)_n + Na]^+$ peaks for n = 1−3. Figure 6b is a zoomed-in look in the mass range of 550−900 amu to show that both the $[(DBZ)_4 + H]^+$ and $[(DBZ)_4 + Na]^+$ peaks are missing (which are expected at roughly 772 and 796 amu, respectively). The disappearance of the "magic-number" tetramer peak in the DBZ mass spectrum suggests that the amide group of CBZ is important in the formation of the CBZ tetramer structure that we detect via mass spectrometry and the structure that we image via STM.

CONCLUSIONS

In summary, we have studied the self-assembly behavior of the active pharmaceutical CBZ and an analog molecule, DBZ, via STM and ESI−MS. Although CBZ is a highly polymorphic molecule in the solid-state, a long-range ordered network of tetramer clusters was the primary structural phase observed upon solution deposition on the Au(111) surface. This tetramer motif that is observed in two dimensions is not a motif that is present in any of the three dimensional solid-state polymorphs of this molecule. Upon removal of the amide group (DBZ), which precludes the formation of strong hydrogen bonds, tetramer formation is precluded. Thus, we posit that the CBZ tetramer is formed by cyclic NH···O hydrogen bonds and the extended network is stabilized by CH···O and $\pi\cdots\pi$ interactions. The mass spectrum of CBZ results in an anomalously intense tetramer peak, which suggests that the tetramer cluster is unusually stable. The formation of tetramers both on the Au(111) surface and as gas-phase ions observed in the mass spectrum suggests that a surface is not required to stabilize the tetramer clusters and that the tetramer clusters likely form in solution. This work may contribute to a fundamental understanding of the relationship between the molecular structure and extended structure and may shed light on the role of the solvent in crystallization, which are research questions of interest to the crystal structure prediction community.

ASSOCIATED CONTENT

Supporting Information

The Supporting Information is available free of charge at https://pubs.acs.org/doi/10.1021/acs.jpcc.9b11466.

Additional mass spectra of CBZ at various solution concentrations and instrument conditions (PDF)

AUTHOR INFORMATION

Corresponding Author

S. Alex Kandel − *Department of Chemistry and Biochemistry, University of Notre Dame, Notre Dame, Indiana 46556, United States;* orcid.org/0000-0001-8191-1073; Email: skandel@nd.edu

https://dx.doi.org/10.1021/acs.jpcc.9b11466
J. Phys. Chem. C 2020, 124, 5213−5219

Authors

Angela M. Silski-Devlin − *Department of Chemistry and Biochemistry, University of Notre Dame, Notre Dame, Indiana 46556, United States*

Jacob P. Petersen − *Department of Chemistry and Biochemistry, University of Notre Dame, Notre Dame, Indiana 46556, United States*

Jonathan Liu − *Department of Chemistry and Biochemistry, University of Notre Dame, Notre Dame, Indiana 46556, United States*

Gwendylan A. Turner − *Department of Chemistry, The College of William and Mary, Williamsburg, Virginia 23187, United States*

John C. Poutsma − *Department of Chemistry, The College of William and Mary, Williamsburg, Virginia 23187, United States;* orcid.org/0000-0002-0085-4079

Complete contact information is available at: https://pubs.acs.org/10.1021/acs.jpcc.9b11466

Notes

The authors declare no competing financial interest.

■ ACKNOWLEDGMENTS

This research was supported by funding from the National Science Foundation (NSF grant no. CHE-1807313). We would like to thank the University of Notre Dame Mass Spectrometry and Proteomics Facility, especially Bill Boggess, for the use of instrumentation and helpful discussions.

■ REFERENCES

(1) Dunitz, J. D.; Bernstein, J. Disappearing Polymorphs. *Acc. Chem. Res.* **1995**, *28*, 193−200.

(2) Bučar, D.-K.; Lancaster, R. W.; Bernstein, J. Disappearing polymorphs revisited. *Angew. Chem., Int. Ed.* **2015**, *54*, 6972−6993.

(3) Chemburkar, S. R.; Bauer, J.; Deming, K.; Spiwek, H.; Patel, K.; Morris, J.; Henry, R.; Spanton, S.; Dziki, W.; Porter, W.; et al. Dealing with the impact of ritonavir polymorphs on the late stages of bulk drug process development. *Org. Process Res. Dev.* **2000**, *4*, 413−417.

(4) Bauer, J.; Spanton, S.; Henry, R.; Quick, J.; Dziki, W.; Porter, W.; Morris, J. Ritonavir: An extraordinary example of conformational polymorphism. *Pharm. Res.* **2001**, *18*, 859−866.

(5) McAfee, D. A.; Hadgraft, J.; Lane, M. E. Rotigotine: The first new chemical entity for transdermal drug delivery. *Eur. J. Pharm. Biopharm.* **2014**, *88*, 586−593.

(6) Rietveld, I. B.; Céolin, R. Rotigotine: Unexpected polymorphism with predictable overall monotropic behavior. *J. Pharm. Sci.* **2015**, *104*, 4117−4122.

(7) Desiraju, G. R. Crystal Engineering: From Molecule to Crystal. *J. Am. Chem. Soc.* **2013**, *135*, 9952−9967.

(8) Corpinot, M. K.; Stratford, S. A.; Arhangelskis, M.; Anka-Lufford, J.; Halasz, I.; Judaš, N.; Jones, W.; Bučar, D.-K. On the predictability of supramolecular interactions in molecular cocrystals—the view from the bench. *CrystEngComm* **2016**, *18*, 5434−5439.

(9) Reilly, A. M.; Cooper, R. I.; Adjiman, C. S.; Bhattacharya, S.; Boese, A. D.; Brandenburg, J. G.; Bygrave, P. J.; Bylsma, R.; Campbell, J. E.; Car, R.; et al. Report on the sixth blind test of organic crystal structure prediction methods. *Acta Crystallogr., Sect. B: Struct. Sci., Cryst. Eng. Mater.* **2016**, *72*, 439−459.

(10) Gutzler, R.; Cardenas, L.; Rosei, F. Kinetics and thermodynamics in surface-confined molecular self-assembly. *Chem. Sci.* **2011**, *2*, 2290.

(11) Conti, S.; Cecchini, M. Predicting molecular self-assembly at surfaces: A statistical thermodynamics and modeling approach. *Phys. Chem. Chem. Phys.* **2016**, *18*, 31480−31493.

(12) Grzesiak, A. L.; Lang, M.; Kim, K.; Matzger, A. J. Comparison of the four anhydrous polymorphs of carbamazepine and the crystal structure of form I. *J. Pharm. Sci.* **2003**, *92*, 2260−2271.

(13) Czernicki, W.; Baranska, M. Carbamazepine polymorphs: Theoretical and experimental vibrational spectroscopy studies. *Vib. Spectrosc.* **2013**, *65*, 12−23.

(14) Arlin, J.-B.; Price, L. S.; Price, S. L.; Florence, A. J. A strategy for producing predicted polymorphs: catameric carbamazepine form V. *Chem. Commun.* **2011**, *47*, 7074−7076.

(15) Popoff, A.; Fichou, D. Immobilization of paracetamol and benzocaine pro-drug derivatives as long-range self-organized monolayers on graphite. *Colloids Surf., B* **2008**, *63*, 153−158.

(16) Iski, E. V.; Johnston, B. F.; Florence, A. J.; Urquhart, A. J.; Sykes, E. C. H. Surface-mediated two-dimensional growth of the pharmaceutical carbamazepine. *ACS Nano* **2010**, *4*, 5061−5068.

(17) Iski, E. V.; Johnston, B. F.; Florence, A. J.; Sykes, E. C. H.; Urquhart, A. J.; Urquhart, A. J. Carbamazepine on a carbamazepine monolayer forms unique 1D supramolecular assemblies. *Chem. Commun.* **2011**, *47*, 9627−9629.

(18) Wasio, N. A.; Quardokus, R. C.; Brown, R. D.; Forrest, R. P.; Lent, C. S.; Corcelli, S. A.; Christie, J. A.; Henderson, K. W.; Kandel, S. A. Cyclic hydrogen bonding in indole carboxylic acid clusters. *J. Phys. Chem. C* **2015**, *119*, 21011−21017.

(19) De Marchi, F.; Cui, D.; Lipton-Duffin, J.; Santato, C.; MacLeod, J. M.; Rosei, F. Self-assembly of indole-2-carboxylic acid at graphite and gold surfaces. *J. Chem. Phys.* **2015**, *142*, 101923.

(20) Liriano, M. L.; Carrasco, J.; Lewis, E. A.; Murphy, C. J.; Lawton, T. J.; Marcinkowski, M. D.; Therrien, A. J.; Michaelides, A.; Sykes, E. C. H. The interplay of covalency, hydrogen bonding, and dispersion leads to a long range chiral network: The example of 2-butanol. *J. Chem. Phys.* **2016**, *144*, 094703.

(21) Mahapatra, M.; Burkholder, L.; Bai, Y.; Garvey, M.; Boscoboinik, J. A.; Hirschmugl, C.; Tysoe, W. T. Formation of chiral self-assembled structures of amino acids on transition-metal surfaces: Alanine on Pd(111). *J. Phys. Chem. C* **2014**, *118*, 6856−6865.

(22) Dou, R.; Yang, Y.; Zhang, P.; Zhong, D.; Fuchs, H.; Wang, Y.; Chi, L. Building chessboard-like supramolecular structures on Au(111) surfaces. *Nanotechnology* **2015**, *26*, 385601.

(23) Chen, C.; Sang, H.; Ding, P.; Sun, Y.; Mura, M.; Hu, Y.; Kantorovich, L. N.; Besenbacher, F.; Yu, M. Xanthine quartets on Au(111). *J. Am. Chem. Soc.* **2018**, *140*, 54−57.

(24) Fenn, J.; Mann, M.; Meng, C.; Wong, S.; Whitehouse, C. Electrospray ionization for mass spectrometry of large biomolecules. *Science* **1989**, *246*, 64−71.

(25) Cooks, R. G.; Zhang, D.; Koch, K. J.; Gozzo, F. C.; Eberlin, M. N. Chiroselective self-directed octamerization of serine: Implications for homochirogenesis. *Anal. Chem.* **2001**, *73*, 3646−3655.

(26) Gozzo, F. C.; Santos, L. S.; Augusti, R.; Consorti, C. S.; Dupont, J.; Eberlin, M. N. Gaseous supramolecules of imidazolium ionic liquids: "magic" numbers and intrinsic strengths of hydrogen bonds. *Chem.—Eur. J.* **2004**, *10*, 6187−6193.

(27) Kennedy, D. F.; Drummond, C. J. Large aggregated ions found in some protic ionic liquids. *J. Phys. Chem. B* **2009**, *113*, 5690−5693.

(28) Brown, R. D.; Coman, J. M.; Christie, J. A.; Forrest, R. P.; Lent, C. S.; Corcelli, S. A.; Henderson, K. W.; Kandel, S. A. Evolution of metastable clusters into ordered structures for 1,1−prime;-ferrocene-dicarboxylic acid on the Au(111) surface. *J. Phys. Chem. C* **2017**, *121*, 6191−6198.

(29) Silski, A. M.; Brown, R. D.; Petersen, J. P.; Coman, J. M.; Turner, D. A.; Smith, Z. M.; Corcelli, S. A.; Poutsma, J. C.; Kandel, S. A. C−H··· O hydrogen bonding in pentamers of isatin. *J. Phys. Chem. C* **2017**, *121*, 21520−21526.

(30) Rutkowski, P. X.; Michelini, M. C.; Gibson, J. K. Gas-phase lanthanide chloride clusters: Relationships among ESI abundances and DFT structures and energetics. *Phys. Chem. Chem. Phys.* **2012**, *14*, 1965−1977.

(31) Chillier, X. F. D.; Monnier, A.; Bill, H.; Gülaçar, F. O.; Buchs, A.; McLuckey, S. A.; Van Berkel, G. J. A Mass Spectrometry and

Optical Spectroscopy Investigation of Gas-phase Ion Formation in Electrospray. *Rapid Commun. Mass Spectrom.* **1996**, *10*, 299−304.
(32) Wong, S. S.; Röllgen, F. W. The effect of a glycerol matrix on the cluster ion formation from salts in secondary ion mass spectrometry. *Int. J. Mass Spectrom. Ion Processes* **1986**, *70*, 135−144.
(33) Zhang, D.; Cooks, R. G. Doubly charged cluster ions $[(NaCl)_m(Na)^2)\ 2^+$: magic numbers, dissociation, and structure. *Int. J. Mass Spectrom.* **2000**, *195*−*196*, 667−684.

https://dx.doi.org/10.1021/acs.jpcc.9b11466
J. Phys. Chem. C 2020, 124, 5213−5219